Signal Design and Processing Techniques for WSR-88D Ambiguity Resolution

Further Investigation

National Severe Storms Laboratory Report

prepared by: M. Sachidananda
with contributions by: D. S. Zrnić and R. J. Doviak

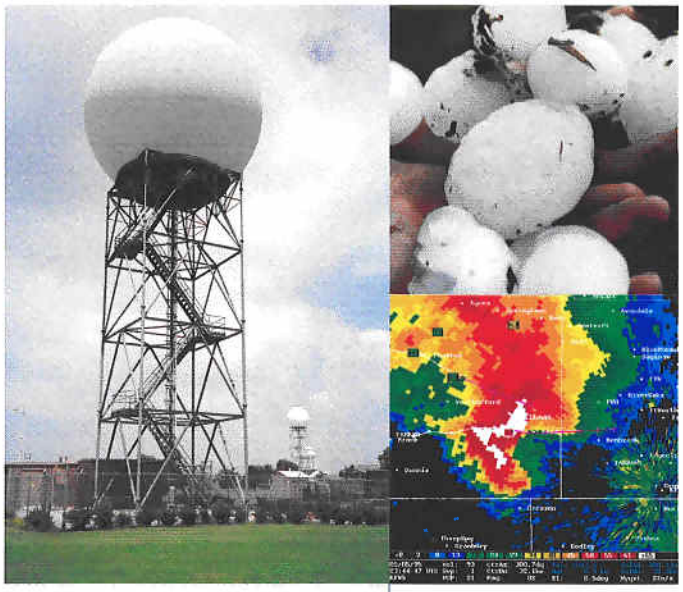

Part 5
October 2001

National Oceanic and Atmospheric Administration
National Severe Storms Laboratory
Norman, Oklahoma 73069

SIGNAL DESIGN AND PROCESSING TECHNIQUES FOR WSR-88D AMBIGUITY RESOLUTION

PART – 5: Further Investigation

National Severe Storms Laboratory Report

prepared by: M. Sachidananda,
with contributions by: D.S. Zrnic and R.J. Doviak

October 2001

NOAA, National Severe Storms Laboratory
1313 Halley Circle, Norman, Oklahoma 73069

SIGNAL DESIGN AND PROCESSING TECHNIQUES FOR WSR-88D AMBIGUITY RESOLUTION
Part-4: Some Investigations.

Contents

ooo000ooo

SIGNAL DESIGN AND PROCESSING TECHNIQUES FOR WSR-88D AMBIGUITY RESOLUTION

Part–5: Further Investigation

1. Introduction

The Radar Operations Center (ROC) of the National Weather Service (NWS) has funded the National Severe Storms Laboratory (NSSL) to address the mitigation of range and velocity ambiguities in the WSR-88D. This is the fifth report in the series that deals with range-velocity ambiguity resolution in the WSR-88D. The first two reports mainly dealt with the uniform PRT transmission and phase coding techniques to resolve the range ambiguity. Although the phase coding techniques do not directly address the velocity ambiguity problem, their capability to separate overlaid echoes allows the use of shorter PRTs which, in turn, diminishes the occurrence of ambiguous velocities. In the third report, we considered the staggered PRT technique and its variants. A significant outcome of the work is a new staggered PRT sequence processing technique in the spectral domain with significantly improved spectral moment estimates, and a clutter filtering technique that recovers velocity information over the entire extended unambiguous velocity interval without any drop-out regions. The only assumption made in the algorithm is that there are no overlaid signals. This necessarily restricts the selection of T_1 (the short PRT segment) to be sufficiently large for a given elevation so that the probability of overlay is small.

After the third report was submitted in July 1999, some more ideas were explored in an effort to further improve the staggered PRT scheme. Specifically, we tried to reduce the velocity estimate errors by optimizing the window weights. We also examined the possibility of extending the unambiguous range from r_{a1} to r_{a2}, by resolving one-overlay situation. The one-overlay situation is one in which only the short PRT can generate

overlaid echoes in the long PRT interval. Exhaustive simulations were carried out to evaluate the performance of the staggered PRT decoding scheme, and determine the limits of spectral moment recovery within acceptable range under various conditions. This information is very useful in developing a data censoring strategy to discard or flag the bad data. The results from all these studies are in Report 4.

There are several points that were left out during the course of the study of the range-velocity ambiguity problem in the WSR-88D. Some of these are addressed in this fifth report. In the SZ phase coding technique, suggested for low elevation angle scans of the WSR-88D radar, an alternative to the magnitude deconvolution, called the substitution method, is proposed by Frush (1999). A comparative study was carried out to evaluate its performance vis-à-vis the magnitude deconvolution proposed by Sachidananda and Zrnic (1999). These results are discussed in Section 2 of this report. Apart from the Section 2, which pertains to the SZ coding technique, the rest of the report is concerned with the staggered PRT technique.

During one of the review meetings concerning the range-velocity ambiguity work, Jim Evans (2001) suggested to examine the possibility of estimating the aliased velocity from the autocorrelation R_1 and de-alias it using R_2, for the staggered PRT technique. On examination, it is found that this indeed is possible in the absence of clutter, and the estimate variance is much lower than using other methods. We have evaluated this technique using simulation and compared it with other methods. The results are presented in Section 3.

In the course of examination of the suggested spectral domain ground clutter filtering technique for the staggered PRT sequence, the theoretical analysis showed a possibility of exact complex reconstruction of the lost signal components. The theory and conclusions arrived at after testing the procedure using simulations is presented in Section 4.

A fifth section deals with the recovery of spectral moments of weather signals that have very narrow spectrum widths overlapping a very strong ground clutter return. Most of our results presented in Report 3 and 4 dealt with weather signals of width 4 m s^{-1}. The specific case of a very narrow width signal (w<1 m s^{-1}) overlapping the clutter requires a

window function with much lower side lobes than that used for larger widths. This is discussed in Section 5.

A new Sigmet processor has been connected (in a passive mode) to the WSR-88D research radar at NSSL. Thus we were able to record some time series data using uniform PRT transmission. Although the staggered PRT is not programmed in yet, we can derive a staggered PRT time series from the uniform PRT sequence by dropping appropriate samples. Further, the uniform sample set can be processed by standard algorithms and the spectral moments compared with those of the staggered set. A comparative study of different data sets has been carried out and some statistics of the standard error has also been generated using the actual radar data. All these results are presented in Section 6.

Finally, there were some lacunae in the suggested vcp-11 scan strategy for the WSR-88D in Report 4. These recommendations are reviewed and revised tables with additional inputs are given in the last section.

2. Magnitude deconvolution and the substitution in SZ-1: a comparison of performance

Sachidananda et al. (1997) proposed the SZ-1 algorithm for retrieving the mean velocity and spectrum width of the weaker of the two overlaid signals from the SZ(8/64) phase encoded sequence of returned echoes. The algorithm uses recohering and magnitude deconvolution. First the stronger signal is removed by a spectral domain notch filter of width equal to ¾ of the total number of spectral coefficients, centered on the stronger signal mean velocity. The remaining ¼ of the spectrum contains two replicas of the weaker signal, which when recohered produce the original signal and symmetrically spaced side bands. The mean velocity, obtained from this time series, is a very good estimate in spite of the side bands presence. There is no bias in the velocity estimate because side bands are symmetric. Nonetheless, the spectrum width is affected by the side bands. To reincorporate the power from the side bands into the main spectral lobe, a magnitude domain deconvolution is carried out before the spectrum width is computed.

Frush (1999) proposed an alternative, called the substitution method. In it, the phase difference between the two replicas available in the remaining ¼ of the spectrum (after notch filtering) is used to reconstruct the deleted replicas of the weaker signal

spectral coefficients. Because the spectrum is a convolution of the signal spectrum with the code spectrum, the sequence of the phase shifts for the replicas progress in predetermined increments, each of which is unique. For the SZ(8/64) coded time series these unique increments can be derived from the code spectrum. The spectrum thus reconstructed by substitution, is transformed to the time domain and recohered to reconstruct the original signal without any side bands. Therefore, both the mean velocity and spectrum width can be computed from it.

The deconvolution operation is a matrix multiplication (i.e., pre-multiply the spectrum matrix with the deconvolution matrix). We also need to compute the autocorrelation $R(1)$ twice, once before the deconvolution to obtain the mean velocity and again after the deconvolution to obtain the spectrum width. This repetition is because the deconvolution procedure increases the estimate variance whenever the spectrum is not "narrow" (see Sachidananda et al. 1998), hence to get a better mean velocity estimate it is necessary to compute the velocity before the deconvolution. The substitution method requires computation of phase differences, comparisons with the code spectrum sequence of phase differences to determine the match, then shift the phase of the spectral replicas by the successive phase difference sequence, and substitution of these replicas in the place where the notch filter was applied. The rest of the computations are the same for the two algorithms.

Both these procedures are developed based on the assumption of a "narrow" spectrum as defined by Sachidananda et al. (1998). If the spectrum is "narrow" both methods are exact and give the same results. The difference in the performance in terms of the estimate variances arises because the "narrow" spectra criterion is not exactly satisfied in actual weather signals, and the noise is always present along with the signal. If the spectral spread is more than $1/8^{th}$ of the Nyquist interval, the replicas in the SZ coded signal spectrum overlap, and the reconstruction is not exact. It is this aspect that is compared here using simulation procedure to generate the statistics of velocity and spectrum width recovery. The SZ-1 decoding algorithm is reproduced here from Sachidananda et al. 1998) to conveniently compare the two methods. The details of the substitution procedure used in this simulation study are also presented before the results are discussed.

2.1 The SZ-1 decoding algorithm

This algorithm was developed for SZ(n/64) coded transmission in the short PRT mode (i.e., the shorter of two PRTs used in the successive scans at the lowest two elevations). The step by step procedure follows (for details of the algorithm and description of math symbols, see Sachidananda et al. (1998), depending on the context = is often used as in a programming language to indicate substitution of a variable into a memory register).

<<< **START** of algorithm (*stand alone mode; **does not** use long PRT data*)

1. Input raw time series E_{1k} ; k=1,2, ... M.
   - The phase switching sequence ψ_k ; SZ(n/M) code.
2. Cohere the 1st trip signal.
   - $E_1 = E_{1k} \exp\{-j\psi_k\}$.
   - 1st trip is coherent; 2nd trip is phase coded by a sequence
     $\varphi_k = n\pi k^2/M$; k=0,1,2,.... M-1.
3. Multiply by von Hann window weights, h_k.
   - $E_1 = E_1 h_k$.
4. Filter the ground clutter.
   - E_1 = GCF(E_1).
5. Cohere the second trip.
   - $E_2 = E_1 \exp\{-j\varphi_k\}$.
6. Autocovariance process E_1 and E_2 to get $\hat{p}_1,\hat{v}_1,\hat{w}_1,\hat{w}_1'$ and $\hat{p}_2,\hat{v}_2,\hat{w}_2,\hat{w}_2'$
   (for the computation of $\hat{w}_1',\hat{w}_2'$ use Eq. 6.27 of Doviak and Zrnic, 1993, and for the computation of $\hat{w}_1,\hat{w}_2$ use Eq. 6.32 of Doviak and Zrnic, 1993).
7. Compute $\hat{w}_1'/\hat{w}_2'$ ratio.
   - if $\hat{w}_1'/\hat{w}_2' > 1$, trip=2, second trip is stronger - process E_2.
   - if $\hat{w}_1'/\hat{w}_2' < 1$, trip=1, first trip is stronger - process E_1.

8. If trip=2, interchange E_1 & E_2, and all the parameters in step number 6.

- with this interchange, E_1 is the time series with stronger signal coherent.
- we need to recover $\hat{p}_2$,$\hat{v}_2$ and $\hat{w}_2$ of the weaker signal.

[Note: The processing steps 9 to 17 are the same for the two cases in step 7 with E_1 replaced by E_2. This is accomplished by step 8, and the trip numbers are restored in the step 18.]

9. Compute spectrum of E_1.

- $S_1' = \text{DFT}\ [\ E_1\ ]$.

10. Notch ($n_w M$) coefficients centered on $\hat{v}_1$ to get S_1 from S_1'.

Note: (a) n_w is not to exceed the maximum permissible value, (1-2n/M).

(b) for SZ(8/64) & SZ(12/64) optimum PNF center location to be computed if trip=1 (i.e. 1st trip stronger) and GCF is applied.

11. Compute the mean power p from the remaining coefficients.

Multiply p by $1/(1-n_w)$ to get mean power estimate $\hat{p}_2$.

12. Compute power ratio $pr = 10 \log_{10}(\hat{p}_1/\hat{p}_2)$ dB.

13. If pr< 25 dB, correct error in $\hat{p}_1$ estimate.

- $\hat{p}_1' = \hat{p}_1 - \hat{p}_2$.
- compute corrected power ratio $\hat{p}r = \hat{p}_1'/\hat{p}_1$.

14. Cohere the weaker signal in S_1.

- $e_1 = \text{IDFT}\ [\ S_1\ ]$
- if trip = 1, $e_2 = e_1 \exp\{-j\varphi_k\ \}$.
- if trip = 2, $e_2 = e_1 \exp\{\ j\varphi_k\ \}$.

15. Compute autocorrelation $R(1)$ for e_2, and compute mean velocity, $\hat{v}_2$.

16. Magnitude deconvolution. (for SZ(8/64) and SZ(16/64) only)

- compute magnitude spectrum, $s_2' = |\ \text{DFT}(e_2)\ |$.
- multiply by the deconvolution matrix, $s_2 = D\ s_2'$.

[The deconvolution matrix, D, is a part of the program. D is pre-computed and supplied to the algorithm, or stored as a

part of the program.]

17. Compute autocorrelation $R(1)$ for s_2, and compute width, $\hat{w}_2$.

18. If trip = 2, interchange parameters ($\hat{p}_1$,$\hat{v}_1$,$\hat{w}_1$) and ($\hat{p}_2$,$\hat{v}_2$,$\hat{w}_2$).

19. Output the 1st and 2nd trip parameters and go to the next sequence.

<<<----------**END** of algorithm

Modifications of the SZ-1 algorithm required by the substitution method.

To use the **substitution** instead of **magnitude deconvolution** in the SZ-1 algorithm, the following steps need to be modified. The steps #1 to #13 are the same. The steps #14 to #17 have to be replaced by the following steps(#14 to #16):

---

14. Reconstruct complete S_1 using substitution (for SZ(8/64) and SZ(16/64) only; details of this step for SZ(8/64) are given in section 2.2).

15. Cohere the weaker signal in S_1.

- e_1 = IDFT [S_1]
- if trip = 1, $e_2 = e_1 \exp\{-j\varphi_k\}$.
- if trip = 2, $e_2 = e_1 \exp\{j\varphi_k\}$.

[Note: This entire step 15 can be replaced by complex deconvolution in the frequency domain, because the corresponding convolution matrix is not singular if the filter function is deleted.]

16. Compute autocorrelation $R(1)$ for e_2, and compute mean velocity, $\hat{v}_2$, and width, $\hat{w}_2$.

The substitution method is based on the observation that if the signal spectrum is "narrow", the spectral replicas of signal modulated with the SZ(8/64) code differ in phase by the amount equal to the phase differences of the code spectral lines. This follows

from the nature of the code, because the eight replicas are obtained from the convolution of the original signal spectrum and the code spectrum. The spectrum of the modulation code $exp(jk^2\pi/8)$, has only 8 uniformly spaced non-zero coefficients with constant amplitudes and the phases $\{\pi/4, \pi/8, -\pi/4, -7\pi/8, \pi/4, -7\pi/8, -\pi/4, \pi/8\}$. Thus for M=64, if the original signal components are in the first 8 coefficients, the sequence of phase difference between the consecutive spectral replicas is $\{-\pi/8, -3\pi/8, -5\pi/8, -7\pi/8, 7\pi/8, 5\pi/8, 3\pi/8, \pi/8\}$. If the original signal coefficients are in the 9^{th} to 16^{th} coefficients, the phase difference sequence would be $\{\pi/8, -\pi/8, -3\pi/8, -5\pi/8, -7\pi/8, 7\pi/8, 5\pi/8, 3\pi/8\}$. Note that the position of the $-\pi/8$ phase difference is the location of the original signal component, and each entry in the sequence is unique. Thus, if we have two adjacent replicas of the modulated spectrum, we can reconstruct the filtered replicas of the spectrum by adding the replicas with appropriate phase shifts. The procedure for reconstructing the spectral replicas is explained next.

2.2 The details of step 14 (substitution method for SZ(8/64))

The spectrum S_1 consists of $M/4$ non-zero coefficients after applying the ¾ notch filter in step #10. Let the indices of these spectral coefficients be k to $(k+M/4-1)$. Note that the indices are cyclic and hence if any index exceeds M, subtract M from it to get the correct index. Of these $M/4$ coefficients, take any two separated by 8, i.e., i^{th} and $(i+M/8)^{th}$, and determine the phase of $S_1(i+M/8)/S_1(i)$. Now, compare this value with the eight values in the sequence, $\{\pi/8, -\pi/8, -3\pi/8, -5\pi/8, -7\pi/8, 7\pi/8, 5\pi/8, 3\pi/8\}$. The position of the closest match in the sequence is taken as the starting phase difference, and the rest of the entries are rotated cyclically to get the rearranged sequence. For example, if the calculated phase difference is closest to $-3\pi/8$, the rearranged sequence would be $\{-3\pi/8, -5\pi/8, -7\pi/8, 7\pi/8, 5\pi/8, 3\pi/8, \pi/8, -\pi/8\}$. Now, the coefficients at spectral indices $(i+nM/8)$; n=0,1,...7, are constructed by adding the phases in the above sequence to $S(i)$, of which the first two are already available. The rest are computed and inserted in the appropriate spectral places in the spectrum. This procedure is repeated for $i= k$ to $k+M/8$ which will reconstruct all the filtered coefficients.

A similar procedure can be followed for SZ(16/64) code.

2.3 Results of simulation and comparison of standard errors

The performance of the SZ-1 decoding algorithm using the magnitude deconvolution and the substitution method, in terms of the standard errors in the mean velocity and spectrum width estimates is obtained from simulation studies. The SZ(8/64) coded time series are simulated with different input velocities, spectrum widths, and overlay power ratios. The spectral parameters are estimated using the SZ-1 algorithm incorporating the deconvolution as well as substitution method. A large number of simulations are carried out to generate the statistics of the error estimates. The standard errors of the mean velocity estimate, v_2, and the spectrum width, w_2, of the weaker signal are compared in Figs. 2.1 and 2.2. The radar parameters used in the simulation are given in the figures. The curves are for w_2=2, 4, 6 and 8 m s^{-1}, respectively, starting with 2 m s^{-1} at the lowest. The continuous curves are for the deconvolution method and the dashed ones are for the substitution method. The curves are smoothed using a 5 point running average filter for clarity. The Fig. 2.1 is for mean velocity error, and Fig. 2.2 is for the spectrum width estimate error. It can be observed from the figures that, whereas the general trend is the same, the deconvolution method gives marginally better estimates than the substitution method, both for the velocity and the spectrum width. This difference is attributed to the manner in which the two methods reconstruct the weaker spectrum when the spectral replicas overlap. If the spectra overlap both methods are not exact but they work reasonably well for a single overlap of the spectral replicas.

2.4 Exact spectral reconstruction if the spectral replicas overlap onece

The substitution (and the deconvolution) procedure is exact only if the spectra are "narrow". If the spectrum spread is more than $1/8^{th}$ of the Nyquist interval, there will be overlapping spectral replicas which produce unequal amplitudes for the coefficients separated by 8 coefficients, and the phase difference will be arbitrary depending on the amplitude and phase of the overlapping signal components. Therefore, in the substitution method we have to compare the measured phase difference with the values in the expected sequence and choose the closest one. This is based on the assumption that one of the coefficients is small compared to the other, so that the phase difference is predominantly due to the stronger of the two overlapped coefficients. This assumption is

reasonably satisfied for the coefficients around the peak of the spectrum, but can lead to wrong phases at the tail ends of the spectrum.

In this section, we examine if it is possible to separate the two overlapping spectra. Further we assume that the spectra are overlapped once only, i.e., the non zero spectral coefficients are spread over $M/4$ coefficients, instead of $M/8$ coefficients. Here, we only give a theoretical analysis of the possibility of exact reconstruction. The additional computation is justified only if it yields substantial improvements in the width estimate. There is no possibility of further improvements in the velocity estimate by improved substitution. The velocity is estimated before the deconvolution in the SZ-1 algorithm, and reconstruction of the complete spectrum is not required for the velocity estimation. It is also mentioned in the report by Sachidananda et al. (1998, page 11, 2nd paragraph) that the velocity estimates worsen if it is obtained from the deconvolved spectrum. In general, any attempt to alter the spectrum results in a higher variance of the velocity estimate.

In order to explain the separation of the overlapped spectra, first we introduce the notation. Let S_1 be the spectrum after the notch filter is applied. For M=64, SZ(8/64) code modulation, and $3M/4$ notch filter width, it consists of only 16 non-zero coefficients. Let two of these non-zero coefficients, separated by $M/8$, be $S_1(i)$ and $S_1(i+M/8)$, and let these two coefficients have two original complex spectral coefficients, a and b, overlapping. Thus, we can write these two as a sum

$$S_1(i) = a \exp(j\phi_1) + b \exp(j\phi_2) ,$$

and

$$S_1(i+M/8) = a \exp(j\phi_2) + b \exp(j\phi_3) . \qquad (2.1)$$

The exponential multipliers are the coefficients of the convolution matrix, therefore, the phases, ϕ_i , i = 1,2,...8, are known. This gives us two equations with two unknowns, a and b which can be solved to obtain

$$a = [S_1(i) \exp(-j\phi_2) - S_1(i+M/8) \exp(-j\phi_3)] / [\exp(j(\phi_1-\phi_2)) - \exp(j(\phi_2-\phi_3))], \qquad (2.2)$$

and

$$b = [S_1(i) \exp(-j\phi_1) - S_1(i+M/8) \exp(-j\phi_2)] / [\exp(-j(\phi_1-\phi_2)) - \exp(-j(\phi_2-\phi_3))] . \qquad (2.3)$$

The only unknown in this procedure is one of the ϕ_i , i = 1,2,...8, to use in place of ϕ_1, ϕ_2, and ϕ_3 . Actually there is only one unknown because we know that the three phases are consecutive phases in the code sequence, hence we have to determine only ϕ_1 and the other two will follow from the sequence.

Now, we have to resort to the same procedure as before to determine the position of the phase difference between the two coefficients in the phase difference sequence $\{\pi/8, -\pi/8, -3\pi/8, -5\pi/8, -7\pi/8, 7\pi/8, 5\pi/8, 3\pi/8\}$. Find the closest match and build the sequence from that point onwards. We can also carry out an amplitude test to determine if the coefficient in question has overlay or not. If the two coefficients, $S_1(i)$ and $S_1(i+M/8)$, have different magnitudes then we know that there is overlay; the phase difference also will deviate from the one corresponding to the convolution code. We can only hope that one of the two overlaid signals is stronger so that we can resolve the correct phase difference. Once the two coefficients, a and b, are solved for, the complete set of 8 coefficients can be reconstructed very easily. This procedure can be applied to all the M/8 pairs present in the spectrum S_1 to restore all the M coefficients.

2.4 Conclusions

In this brief discussion, the magnitude deconvolution and the substitution methods are compared with respect to their performance in terms of the standard errors in the velocity and width estimates. Although both the velocity and width estimate errors are compared, it must be noted that the deconvolution method is used only for width estimation. The velocity estimation does not require the deconvolution. However, in the substitution method the velocity and width are estimated after the substitution, and hence we have compared the velocity errors also. Both methods perform well even if the spectra are not "narrow", but the deconvolution method performs marginally better, both with respect to the velocity and the width estimates.

3. Mean velocity estimation in the staggered PRT technique

Here, we describe the staggered PRT scheme briefly before we embark on a discussion of the method of processing. In the staggered PRT technique (Zrnic and Mahapatra 1985), two different pulse spacings, T_1 and T_2, are used alternately. Then,

alternate pairs of return samples are used to compute autocorrelation estimates, R_1 at lag T_1 and R_2 at lag T_2. The velocity is estimated from the phase difference between the two using the formula,

$$\hat{v} = \lambda \, arg(R_1 R_2^*) / [4\pi(T_2 - T_1)] \, . \qquad (3.1)$$

Thus, the difference in PRT, (T_2-T_1), determines the unambiguous velocity, v_a, for the staggered PRT technique and is given by

$$v_a = \lambda / [4(T_2 - T_1)] \; ; \; T_1 < T_2 \, . \qquad (3.2)$$

Zrnic and Mahapatra (1985) suggest a testing procedure to estimate mean velocity and signal power for echoes received within the time delay (T_1+T_2). In theory, this seems to be possible because the overlaid signals in any two consecutive samples are from two different ranges, and therefore are uncorrelated. Thus, the expected value of the overlaid signal contribution to the autocorrelation is zero, and the effective unambiguous range becomes

$$r_a = c(T_1+T_2)/2. \qquad (3.3)$$

Eq. (3.1) and (3.3) suggest that the staggered PRT is equivalent to a uniform PRT = (T_1+T_2) for the unambiguous range, and a uniform PRT = (T_2-T_1) for the unambiguous velocity; each can be selected independently. However, the practical utility of this scheme is limited due to the quality of estimates. The overlaid signal increases the variance of the estimates because it acts as noise. Thus, the ratio of the overlaid signal powers is the equivalent signal-to-noise ratio (SNR), and for a reasonable accuracy of the estimates, the unwanted signal has to be at least 3 dB below the desired signal power.

Let $r_{a1} = cT_1/2$, and $r_{a2} = cT_2/2$, such that $r_a = r_{a1} + r_{a2}$. If r_{a1} is chosen sufficiently large so that no echoes are received from ranges greater than r_{a1}, then the problem of overlaid echoes could be eliminated. For weather radars, r_{a1} would have to be 460 km (for 0.5 deg. elevation scan), but this would degrade the variance of the estimates

considerably. Thus, the practical limit for r_{a1} is smaller than 460 km unless some means of separating the overlaid signals is employed. It is possible to extend the unambiguous range to r_{a2} with some additional processing to resolve the one-overlay (i.e., alternate samples only have overlaid echoes) in some of the range locations.

It is shown by Zrnic and Mahapatra (1985), that the standard error in the velocity estimate increases as the ratio $\kappa = T_1/T_2$ approaches unity, and a good choice is κ =2/3. Thus, in practice, the unambiguous range and unambiguous velocity are restricted indirectly via the estimate accuracy. However, compared to the uniform PRT, it is possible to achieve a much larger r_a and v_a, because the limiting equation is $v_a r_{a1}$ equals $[(\kappa+1)/(1-\kappa)]c\lambda/8$ for the staggered PRT scheme without the overlay.

An alternative to the estimator (3.1), which results in a much lower standard error in the velocity estimate, is to use the phase of $R(T_1)$ for velocity estimation (aliased) and $R(T_2)$ for dealiasing or unfolding. If the ground clutter and overlay are not present, a pulse pair estimation of autocorrelations, $R(T_1)$ and $R(T_2)$, can be used for the estimation of spectral moments. The velocity estimator using the difference in phases of $R(T_1)$ and $R(T_2)$, (Eq. 7 of Zrnic and Mahapatra 1985), has a larger standard error because it uses the difference of two estimates. Sirmans et al. (1976) suggest use of either one of the autocorrelations for velocity estimation.

In our procedure, to obtain the correct velocity, we first compute two velocities, v_1 and v_2, using the phases of $R(T_1)$ and $R(T_2)$, from

$$v_1 = -\lambda \arg\{R(T_1)\} / (4\pi T_1),$$

and

$$v_2 = -\lambda \arg\{R(T_2)\} / (4\pi T_2). \qquad (3.4)$$

Now, assuming occurrence of one time aliasing, the possible velocities from the first estimate are v_1, and $(v_1 + 2v_{a1})$, or $(v_1 - 2v_{a1})$, whichever falls in the interval $\pm v_a$, and from the second estimate we have v_2, $(v_2 + 2v_{a2})$, and $(v_2 - 2v_{a2})$, where v_{a1} and v_{a2} are the unambiguous velocities corresponding to the PRTs, T_1 and T_2. Note that it is sufficient to consider a one-time aliasing for κ=2/3, because $v_a = 2v_{a1} = 3v_{a2}$. In these two sets of possible velocities, only one velocity, the correct one is common to both sets; it can be easily selected after comparison. In general, the velocities are estimates with certain

amount of error, hence we select the two closest, and then pick the corresponding value from the first set. The values from the first set have lower variances than the ones from the second set, because of the shorter PRT. This dealiasing procedure performs the best for κ=2/3, because the difference between the estimated velocities, $|v_1 - v_2|$, is the largest whenever there is aliasing. For effective dealiasing this separation must be larger than the standard error in the estimates. Thus, from the point view of large separation between these values κ=2/3 is also the best choice.

It can be inferred that for large signal spectrum width this unfolding technique is likely to fail (as do all other techniques), because the standard error increases with spectrum width. Therefore, the maximum width for which the unfolding is effective will be a certain fraction of the unambiguous velocity, but it is also a function of the number of staggered PRT samples, because the standard error decreases with increasing number of samples. We define a parameter called *loss* as the ratio of the number of times the unfolding failed to the total number of simulations. Sirmans et al. (1976) call this *loss* a "detection error rate" and compute it for staggered ratios ¾ and 4/5. In our simulation, the input velocity is varied uniformly over the entire $\pm v_a$ interval. The *loss* parameter is shown as a function of the normalized spectrum width in Fig. 3.1, where we have used 40 staggered PRT samples (approximately the same dwell time as in vcp-11 of WSR-88D) to generate simulated time series data for the figure. The PRT in the simulation is T_u = 0.61 ms with a v_a = 45.08 m s^{-1}. For M=40, the limit is about $w_{max} = 0.2v_a$, at which the *loss* is about 10%; i.e., the velocity is not correctly dealiased in 10% of the total number of simulations (about 2000 simulations). The *loss* is nearly zero up to about $w = 0.14v_a$ and then starts increasing rapidly. In the simulation study, the input velocities are spread over 90% Nyquist interval uniformly, leaving out the extreme ends. There is always velocity aliasing at the extreme ends that increases the *loss* by about 2% if 100% of the Nyquist interval is included. It is not included because this 2% does not reflect the performance of the dealiasing procedure. Our simulation results are consistent with the theoretical computations by Sirmans et al. (1976); their values of normalized spectrum width at which catastrophic errors occur are about twice as large as ours mainly because the number of samples in their computations is 2.5 times larger than herein.

A third alternative is to use the reconstructed uniform time series and use magnitude deconvolution procedure delineated in Report 3 (Sachidananda et al. 1999). In this procedure, the time series is made uniform with a period $T_u = T_1/2$ (for κ=2/3), by inserting zeros in place of the missing samples. This time series can be looked at as a product of the full time series and a code sequence of zeros and ones; zeros in place of missing samples and 1s in place of actual staggered PRT samples. The spectrum of this uniform time series is a convolution of the signal spectrum with the spectrum of the code, which has only five non-zero coefficients. Thus, the convolution produces a spectrum with five replicas of the original spectrum separated by $N/5$ coefficients, where N is the number of uniform samples. A magnitude deconvolution procedure can be used to restore the spectrum to the original shape, provided it is "narrow" ("narrow" spectrum is defined in Report 3). One can use this reconstructed magnitude spectrum to compute $R(T_u)$ from which we can get the velocity. This does not require unfolding provided T_u is chosen small enough.

From simulation we evaluated the standard errors in the velocity estimate using four methods. These are: (a) velocity from $R(T_u)$, i.e., uniform samples at intervals T_u, (b) velocity from $R(T_1)$ dealiased with the help of $R(T_2)$, (c) velocity from magnitude deconvolution, and (d) velocity from $\arg\{R(T_1)/R(T_2)\}$. We call the method (b) the staggered PRT pulse pair (ST) method. The various methods are compared in Fig. 3.2. Curve (a), the ideal case where all the samples at intervals T_u are available, is given for reference. The dwell time for all estimates is the same. The values are obtained using simulated time series and estimation of velocities by three different algorithms on the same (staggered PRT) time series. The simulation parameters are indicated in the figure. It is clearly seen that, of the staggered schemes, the method (b) gives the best estimate (curve # b in the figure), followed by (c) and (d).

The staggered PRT one-overlay resolution algorithm (henceforth labeled STO) presented in Report 4 uses the method-(c) if there is no clutter or the overlay. Because the staggered PRT pulse pair algorithm (method-(b)) performs better than the method-(c) in the absence of the ground clutter and the overlay, it is appropriate to replace the method-(c) by method-(b) in the overall schematic of the algorithm given in pages 34-36, Report 4. It is also important to change the thresholds on p_1/p_2 used for channeling the

computation, because the method-(b) performs differently than the method-(c). We have evaluated the ability of the staggered PRT pulse pair algorithm ST to estimate velocity in the presence of one-overlay. The largest p1/p2 ratio for which the pulse pair algorithm is effective in the presence of overlay is determined from simulations; this value is used in the algorithm to switch processing between the pulse pair algorithm ST and the overlay resolution algorithm STO. Because the algorithm is suggested only for the three elevations (2.4°, 3.35°, and 4.3°) of the WSR-88D vcp-11 (see Section 7), we have evaluated the *% loss* and $sd(v)$ as a function of the overlay power ratio, p_2/p_1, using the PRTs proposed for these three elevations. Simulations were carried out for four different spectrum widths of the signal, keeping the overlay signal spectrum width constant (w_2=4 m s^{-1}). The *loss* is nearly independent of the overlay signal spectrum width, w_2, hence, it is kept constant. The parameter *loss* is the number of times the velocity unfolding failed in 2020 simulations, with velocities spread over the entire Nyquist interval, expressed as a percentage. The $sd(v)$ is computed excluding the outliers (i.e., only the correctly unfolded velocity values are included).

Figs. 3.3 to 3.5 show the results of simulations for the three elevations, 2.4°, 3.35°, and 4.3°, respectively. It is apparent that as we decrease T_u (or increase v_a), the *loss* decreases up to a point and then reaches a limit. Note that all *loss* traces are more or less the same in Fig. 3.5 for all widths, but are spaced in Fig. 3.3. If we can tolerate a 10% *loss* for the weaker signal velocity, we can use a 6 dB cut-off for the overlay power ratio, i.e., apply the staggered PRT pulse pair algorithm ST to retrieve velocities of both signals if $|p_2/p_1| < 6$ dB. If it is larger than 6 dB, then we need the overlay resolution algorithm STO to recover the weaker signal velocity. The stronger signal velocity is always recoverable by applying the pulse pair algorithm (ST). Depending on the PRTs (dictated by the elevation angle) and the tolerable *loss,* the 6 dB limit can be lowered to 3 dB. An alternate choice could be 0 dB, in which case the stronger signal would always be processed by the ST pulse pair algorithm and the weaker one by the overlay resolution algorithm STO.

4. Clutter filtering and bias correction in the staggered PRT technique

A spectral domain clutter filtering and bias correction scheme is suggested by Sachidananda et al. (1999, Report 3). There the spectral coefficients of the weather signal, partially lost in the process of clutter filtering, are restored in amplitude using a magnitude deconvolution and multiplication by a coefficient determined from an approximate *initial* estimate of the velocity. During the course of reviewing this procedure, we found that it is possible to restore the complex coefficient exactly provided the spectrum is "narrow" as defined in the above referenced report. But, if the "narrow" spectra assumption is not valid then these two methods, viz., the magnitude only restoration and the exact complex restoration, behave somewhat differently with respect to the velocity estimate errors. It also requires more computation to restore the complex coefficients. Here we only give the mathematics of complex restoration procedure, and state the conclusions arrived at from simulation study. No simulation results are presented.

4.1. Restoration of the complex spectral coefficient and bias correction

The clutter filtering procedure is explained in the paper Sachidananda and Zrnic (2000), without the bias correction procedure, and the magnitude only restoration is explained in the Report 3 (Sachidananda et al. 1999). Here we shall use the same notation as in Report 3. To explain the complex coefficient restoration, let us start with Eq.(3.7), of Sachidananda et al. (1999)

$$\mathbf{V_r} = \mathbf{C_r}\,\mathbf{E_r}\,, \tag{4.1}$$

where $\mathbf{E_r}$ is the rearranged matrix of signal plus the clutter spectrum. Similarly, $\mathbf{C_r}$ is the rearranged convolution matrix, and $\mathbf{V_r}$ is the rearranged signal spectrum matrix after convolution. Assume that the ground clutter is around zero Doppler and the signal spectrum is "narrow". With this assumption, the first few coefficients in the first row and last few coefficients in the last row of $\mathbf{E_r}$ contain ground clutter. The non-zero signal coefficients are spread over only $N/5$ contiguous coefficients row wise; the position being determined by the mean velocity of the signal. Thus in any column of $\mathbf{E_r}$ a maximum of

two coefficients can be non-zero. Now, the convolution operation indicated by Eq. (4.1) spreads the clutter and the signal power present in each column of $\mathbf{E_r}$ into all the coefficients of the same column of $\mathbf{V_r}$. There is no shifting of the power from one column to another. Therefore, it is sufficient to consider one column of $\mathbf{V_r}$ and $\mathbf{E_r}$ to understand the signal restoration procedure. Let, the first column of $\mathbf{E_r}$ be $\mathbf{E_1} = [a, 0, 0, b, 0]^t$, where a is the clutter coefficient, and b is the signal coefficient; both complex. After the convolution, the first column of $\mathbf{V_r}$, **A,** is given by

$$\mathbf{A} = \mathbf{C_r}\,\mathbf{E_1} = a\,\mathbf{C_1} + b\,\mathbf{C_4}\,, \tag{4.2}$$

where $\mathbf{C_1}$ and $\mathbf{C_4}$ are the 1st and 4th columns of the convolution matrix, $\mathbf{C_r}$. After the clutter filtering (Eq. 3.11 of Sachidananda et al. 1999) the first column of $\mathbf{V_f}$ can be written as

$$\mathbf{B} = \mathbf{A} - \mathbf{C_1}^{t*}\mathbf{A}\mathbf{C_1}\,. \tag{4.3}$$

Substituting for **A** in (4.3) and simplifying, we can reduce it to

$$\mathbf{B} = b(\mathbf{C_4} - \mathbf{C_1}^{t*}\mathbf{C_4}\mathbf{C_1}). \tag{4.4}$$

Note that the clutter coefficient, a, is completely deleted by the clutter filtering, but the signal coefficient, b, is multiplied by a complex known vector. Now, to get back the signal vector, $b\mathbf{C_4}$ present in **A**, we carry out the matrix operation given by

$$b\mathbf{C_4} = (\mathbf{C_4}^{t*}\,\mathbf{B}\,\mathbf{C_4}) / (1 - |\,\mathbf{C_1}^{t*}\mathbf{C_4}\,|). \tag{4.5}$$

This procedure is carried out on the first few columns of $\mathbf{V_f}$ from which clutter is filtered to restore the signal vector.

In this illustration we have assumed that the signal coefficient is in the 4th position in $\mathbf{E_1}$. In general the position of the signal coefficient can be any one of the five, hence a general expression can be written as

$$b\mathbf{C}_k = (\mathbf{C}_k^{t*}\,\mathbf{B}\,\mathbf{C}_k) / (1 - |\,\mathbf{C}_1^{t*}\mathbf{C}_k\,|^2), \qquad (4.6)$$

where k is the position of the signal coefficient which is determined from the *initial* velocity estimate. The index k can be different for different columns of $\mathbf{V_f}$ depending on the *initial* velocity. The *initial* velocity is estimated using the magnitude deconvolution procedure on the filtered spectrum, $\mathbf{V_f}$, before restoring the signal components lost during the clutter filtering. For the last few columns of $\mathbf{V_f}$, the clutter coefficient is in the last row, hence $\mathbf{C_1}$ is replaced by $\mathbf{C_5}$ in (4.6) while restoring the signal in these columns. Note that in (4.6) the denominator is zero if k =1, which corresponds to the signal having near zero Doppler. The signal is completely filtered out, and the numerator also would be zero in this case. In the actual radar time series processing, however, the numerator would not be zero because the signal spread is not "narrow" in the strict sense. Thus, we cannot restore the signal if the Doppler is near zero as in the previous method.

If the assumption of "narrow" spectra is strictly valid, then both methods of signal restoration, viz., the magnitude only restoration and the complex restoration, are exact, and give the same spectral moment estimates. However, if the spectra are not "narrow" the two methods differ in performance to some extent. The magnitude restoration performs slightly better than the complex domain restoration in the presence of overlapping spectral replicas, and also requires less computation. We have examined the performance of these two methods using simulated time series, however, no results are presented because the complex restoration did not fare better than the magnitude only restoration explained in Report 3. The results for the magnitude only restoration are available in that report.

5. Ground clutter filtering and the window: some considerations

The ground clutter is usually present in the lower elevation scans approximately in the in the first 20 km from the radar. At elevations higher than about 5° the ground clutter is not a serious problem. The WSR-88D specifies a 50 dB rejection for the ground clutter (at 0.5° and 1. 5° elevation) with a spectrum width of 0.28 m s^{-1} centered on zero Doppler. We use this width for the ground clutter in our simulation study, and use clutter-